

Dipole-Dipole interaction in photonic crystal nanocavity

Yong-Gang Huang,^{1,2,3} Gengyan Chen,¹ Chong-Jun Jin,¹ W. M. Liu,³ and Xue-Hua Wang^{1*}

¹State Key Laboratory of Optoelectronic Materials and Technologies,
Sun Yat-sen University, Guangzhou 510275, China

²College of Physics Science and Information Engineering, Jishou University, Jishou 416000, China and

³Beijing National Laboratory for Condensed Matter Physics,

Institute of Physics, Chinese Academy of Sciences, Beijing 100190 China

(Dated: August 25, 2018)

Dipole-dipole interaction between two two-level ‘atoms’ in photonic crystal nanocavity is investigated based on finite-difference time domain algorithm. This method includes both real and virtual photon effects and can be applied for dipoles with different transition frequencies in both weak and strong coupling regimes. Numerical validations have been made for dipoles in vacuum and in an ideal planar microcavity. For dipoles located in photonic crystal nanocavity, it is found that the cooperative decay parameters and the dipole-dipole interaction potential strongly depend on the following four factors: the atomic position, the atomic transition frequency, the resonance frequency, and the cavity quality factor. Properly arranging the positions of the two atoms, we can acquire equal value of the cooperative decay parameters and the local coupling strength. Large cooperative decay parameters can be achieved when transition frequency is equal to the resonance frequency. For transition frequency varying in a domain of the cavity linewidth around the resonance frequency, dipole-dipole interaction potential changes continuously from attractive to repulsive case. Larger value and sharper change of cooperative parameters and dipole-dipole interaction can be obtained for higher quality factor. Our results provide some manipulative approaches for dipole-dipole interaction with potential application in various fields such as quantum computation and quantum information processing based on solid state nanocavity and quantum dot system.

PACS numbers: 42.50.Ct, 34.20.-b, 37.30.+i

I. INTRODUCTION

Since Purcell predicted spontaneous emission rate could be changed by electromagnetic environment in 1946 [1], the effect of electromagnetic field on radiation properties has been thoroughly investigated [2–10], and classified in the category of cavity quantum electrodynamics (QED). Characteristics of QED have been greatly investigated both theoretically and experimentally [11–16], and many kinds of devices [17, 18] based on this theory have been developed. Concepts such as enhanced and inhibited spontaneous emission [4, 5], reversible spontaneous emission [8], photon blockade [13], micromasers [19], low threshold lasers [20, 21], etc., have become very familiar.

Dipole-dipole interaction could also be greatly modulated by the electromagnetic environment. Photon emitted by one dipole could be absorbed by the other or vice versa. The strength of interaction is decided by photon emission, transmission and absorption. Many different kinds of electromagnetic environment can be used to control or change these characteristics, such as vacuum [3, 22–25], optical cavities [26–29], optical lens [30], dielectric droplet [31], photonic materials [32–38], metal surface [39–43], metamaterial [44, 45] and so on. For example, optical lens and waveguide have been designed to collect the emission photon and transfer it to the other dipole. Optical cavity or metal surface can enhance the emission or absorption rate roughly by the ratio of quality factor Q and the mode volume V .

Photonic crystal nanocavity is one of the promising platform to investigate dipole-dipole interaction, because local coupling strength of dipole and photon can be tailored and integrated to photonic crystal waveguide is extremely convenient. High quality factor $Q = 2.5 \times 10^6$ and small mode volume $V \sim (\lambda/n)^3$ have been realized for photonic crystal cavity [46]. Numerical investigations show that ultra-high quality factor with $Q \sim 10^9$ can be designed through finely tuning the scatters around the cavity with little change of the mode volume [47]. Furthermore, static and ultra fast dynamic control of the cavity frequency and the quality factor have been achieved [48–52]. On the other hand, temperature [9], strain [53], electric field [54], magnetic field [55, 56] are much suitable for fine tuning the energy levels of dipoles located at certain position in solid system.

Recent studies show that this kind of interaction could be used to implement quantum entanglement preparation and quantum information processing [57–64], cooperative radiation [28, 65], Förster energy transfer [66, 67], dipole nanolaser [68], and so on. Furthermore, some novel quantum phenomena [69–73] has been found. All of these applications and phenomena are related to the cooperative decay parameters or dipole-dipole interaction potential. According to Eq. (8c), dipole-dipole interaction potential can be got through the cooperative decay parameters.

In the previous theoretical studies, mode-expansion method [23, 26, 27, 30–32] or Green function method [29, 62–64, 74] is often adopted to investigate this cooperative decay parameters. These two methods work well for

electromagnetic environment with perfect boundary condition. Because of the extremely complexity of finding eigen-mode, mode-expansion method can be used only for simple case such as vacuum or planar cavity. Besides, the exact analytic Green function is also hard to be obtained for complex electromagnetic environments. Numerical method is necessary for studying this kind of interaction in photonic crystal nanostructure.

In this paper, we put forward a simple numerical method to investigate dipole-dipole interaction in photonic crystal nanocavity through finite-difference time domain algorithm (FDTD). We calculate the collective and individual radiation rates of classical dipoles by directly solving Maxwell's equations in real space with a free-space boundary condition. By using the result of two dipoles radiation rate minus the sum of the two individual radiation rates, we get the cooperative decay parameters and dipole-dipole interaction potential. A similar method has been used for local density of photonic states calculation [75–77]. It is direct for structures with arbitrary shape and physical quantities such as radiation power at different frequencies can be got in a single simulation run. Numerical results in vacuum and planar conductor cavity show that our method works well for this kind of investigation. For dipoles located in photonic crystal cavity, the strength of dipole-dipole interaction depends heavily on the following four factors: the atomic position, the transition frequency, quality factor, mode volume and the cavity frequency. Effect of these factors on the interaction strength are also shown.

This paper is organized as follows: In Sec. II, we give the model of dipole-dipole interaction with some illuminations. Numerical method is presented in Sec. III. Validation of this method is presented in Sec. IVA for dipoles in vacuum and in planar microcavity. In Sec. IVB, applying our method to photonic crystal nanocavity, we investigate the effect of the atomic position, the transition frequency, quality factor and the cavity frequency on the dipole-dipole interaction strength. In Sec. V, we give a brief conclusion.

II. MODEL

Schematic diagram of dipole-dipole interaction is illustrated in Fig. 1. There are two two-level ‘atoms’ A and B located at \mathbf{r}_A and \mathbf{r}_B respectively and they both interact with the electromagnetic field with eigen frequency ω_n . The Atom A (B) has two states, the ground state $|g_A\rangle$ ($|g_B\rangle$) and the excited state $|e_A\rangle$ ($|e_B\rangle$), with a transition frequency ω_A (ω_B). The Hamiltonian of the system in the rotation wave approach reads [78]:

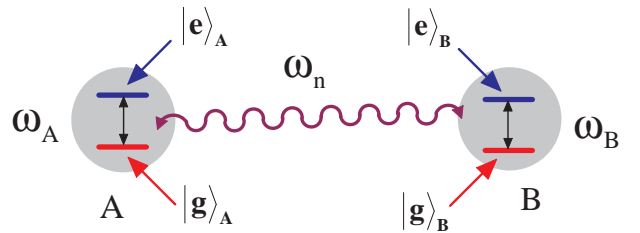


FIG. 1: (Color online). Schematic diagram of dipole-dipole interaction. Consider two two-level ‘atoms’ A and B. Atom A (B) has two states, the ground state $|g_A\rangle$ ($|g_B\rangle$) and the excited state $|e_A\rangle$ ($|e_B\rangle$), with a transition frequency ω_A (ω_B). Atom A is in the excited state $|e_A\rangle$ and atom B is in the ground state $|g_B\rangle$. They both interact with electromagnetic field with eigen frequency ω_n . Analogous to the process of Lamb shift where both virtual and real photon exchange between the atom and the quantum electromagnetic field take effect, photon exchange between the two atoms contribute to dipole-dipole interaction.

$$\begin{aligned}
 H &= H_0 + V, \\
 H_0 &= \hbar \sum_{i=A,B} \omega_i |e_i\rangle \langle e_i| + \hbar \sum_n \omega_n a_n^\dagger a_n, \\
 V &= \hbar \sum_{i=A,B} \sum_n [g_n(\mathbf{r}_i) a_n^\dagger |g_i\rangle \langle e_i| + c.c.]. \quad (1)
 \end{aligned}$$

where a_n^\dagger and a_n are, the photonic creation and annihilation operators, ω_n is the frequency of the eigen mode of the electromagnetic field, $g_n(\mathbf{r}_i) = i\omega_j(2\epsilon_0\hbar\omega_n)^{-1/2}\mathbf{E}_n(\mathbf{r}_i)\cdot\mathbf{u}_i$ ($i = A, B$), is the coupling coefficient, $\mathbf{E}_n(\mathbf{r})$ is the eigen mode, \mathbf{u}_i is the transition dipole moments of atoms i , and ϵ_0 is the vacuum permittivity. In Eq. (1), H_0 is the noninteracting Hamiltonian, and V represents the interaction between dipole and electromagnetic field. There are three states for the system considered: (1) atom A is in the excited state, and atom B is in the ground state, without any photon, i.e., $|a\rangle = |e_A, g_B, 0\rangle$, (2) atom B is in the excited state, and atom A is in the ground state, without any photon, i.e., $|b\rangle = |g_A, e_B, 0\rangle$, (3) both atom A and atom B are in the ground state, with a photon of frequency ω_n , i.e., $|c_n\rangle = |g_A, g_B, 1_n\rangle$.

The initial state is prepared in $|a\rangle$. Then, the state of the system evolves as

$$|\psi(t)\rangle = a(t)|a\rangle + b(t)|b\rangle + \sum_n c_n(t)|c_n\rangle \equiv U(t)|a\rangle. \quad (2)$$

where $U(t)$ is the evolution operator and $a(t) = \langle a|U(t)|a\rangle$, $b(t) = \langle b|U(t)|a\rangle$, $c_n(t) = \langle c_n|U(t)|a\rangle$. To derive the equation for the atom-field dynamics nonperturbatively, the resolvent operator $G(z) = 1/(z - H)$ is adopted [79]. The corresponding advanced and retarded

propagators are $G^\pm(E) = \lim_{\eta \rightarrow 0^+} G(E \pm i\eta)$. Then the evolution operator can be expressed by

$$U(t) = \int_{-\infty}^{+\infty} d\omega [G^-(\omega) - G^+(\omega)] \exp(-i\omega t) / 2\pi i. \quad (3)$$

The dynamic properties of this system are governed by $G_{aa}^\pm(\omega)$ and G_{ba}^\pm . The matrix elements of the resolvent reads

$$\begin{aligned} (z - \hbar\omega_A)G_{aa} &= 1 + \sum_n V_{ac}G_{ca}, \\ (z - \hbar\omega_B)G_{ba} &= \sum_n V_{bc}G_{ca}, \\ (z - \hbar\omega_n)G_{ca} &= V_{ca}G_{aa} + V_{cb}G_{ba}. \end{aligned} \quad (4)$$

where $G_{aa} = \langle a|G(z)|a\rangle$, $G_{BA} = \langle b|G(z)|a\rangle$, $G_{ca} = \langle c_n|G(z)|a\rangle$ and $V_{ac} = V_{ca}^* = \langle a|V|c\rangle$, $V_{bc} = V_{cb}^* = \langle b|V|c\rangle$

Eliminating G_{ca} , we have

$$\begin{aligned} G_{aa}(z) &= (z - \hbar\omega_B - W_{BB}(z)) / \Xi, \\ G_{ba}(z) &= W_{BA}(z) / \Xi. \end{aligned} \quad (5)$$

Ξ is given by

$$\Xi = [z - \hbar\omega_A - W_{AA}][z - \hbar\omega_B - W_{BB}] - W_{AB}W_{BA} \quad (6)$$

The local coupling between atom and the field (W_{AA}, W_{BB}) or the dipole-dipole coupling between atom A and atom B (W_{AB}, W_{BA}) are denoted by

$$W_{ij}(z, \mathbf{r}_i, \mathbf{r}_j) = \hbar \sum_n \frac{g_n^*(\mathbf{r}_i)g_n(\mathbf{r}_j)}{z - \hbar\omega_n}. \quad (7)$$

Clearly, these terms can be written as

$$W_{ij}^\pm(\hbar\omega, \mathbf{r}_i, \mathbf{r}_j) = \hbar [\Delta_{ij}(\omega, \mathbf{r}_i, \mathbf{r}_j) \mp i \frac{\Gamma_{ij}(\omega, \mathbf{r}_i, \mathbf{r}_j)}{2}], \quad (8a)$$

$$\Gamma_{ij}(\omega, \mathbf{r}_i, \mathbf{r}_j) = 2\pi \sum_n g_n^*(\mathbf{r}_i)g_n(\mathbf{r}_j)\delta(\omega - \omega_n), \quad (8b)$$

$$\Delta_{ij}(\omega, \mathbf{r}_i, \mathbf{r}_j) = \frac{1}{2\pi} \oint \int_0^{+\infty} dz \frac{\Gamma_{ij}(z, \mathbf{r}_i, \mathbf{r}_j)}{\omega - z}. \quad (8c)$$

To better understand the physics underlying of these equations, we make some illumination. We are able to self-consistently determine the roots of $\Xi = 0$ (Eq. (6)). The real parts are corresponding to the energy levels of these two atoms and the imaginary parts are the lifetime. Different from the usual Markov approximation method where W_{ij} ($i, j = A, B$) are independent of ω and have been replaced by their approximate value $W_{ii}(\omega_i)$

and $W_{ij}((\omega_i + \omega_j)/2)$, this method is non-Markov and this self-consistent process can give the rigorous dipole-dipole coupling. We can also make use of the Markov approximation values W_{ij} ($i, j = A, B$) in Eq. (6) and get the same results as usual. However, for complex electromagnetic environment such as photonic crystal or photonic crystal nanocavity, W_{ij} may vary sharply around some frequency and non-Markov is necessary. Owing to W_{ij} , equation. (6) also shows that both the energy level and the lifetime of the states are splitting. Different coupling W_{ij} makes different energy level splitting and different lifetime splitting. Dipole blockade, which have been widely investigated in quantum information processing needs large energy gap. Efficient superradiant emission, steady state entanglement preparation and fast Förster energy transfer needs large lifetime splitting. Inspired by these novel application, accurate values for W_{ij} are expected. Furthermore, equation (7) shows that all of the photonic eigen modes contribute to the local coupling and dipole-dipole interaction and both real and virtual photon effects have been taken into account.

Insert $g_n(\mathbf{r}_i) = i\omega_i(2\varepsilon_0\hbar\omega_n)^{-1/2}\mathbf{E}_n(\mathbf{r}_i)\cdot\mathbf{u}_i$ ($i = A, B$) into Eq. (8b) for $i \neq j$, and define $s_{i,j}(\omega) \equiv \pi\omega_i\omega_j\mathbf{u}_i\mathbf{u}_j/(\varepsilon_0\hbar\omega)$ ($i = A, B$), where u_i and $\hat{\mathbf{u}}_i$ are the size and the unit vector of transition dipole \mathbf{u}_i . Then, the cooperative decay parameters reads:

$$\Gamma_{ij}(\omega, \mathbf{r}_i, \mathbf{r}_j) = s_{i,j}(\omega) \sum_n \mathbf{E}_n^*(\mathbf{r}_i)\cdot\hat{\mathbf{u}}_i\mathbf{E}_n(\mathbf{r}_j)\cdot\hat{\mathbf{u}}_j\delta(\omega - \omega_n). \quad (9)$$

For simplicity, we denote $\Gamma_{ij}(\omega)$ and $\Delta_{ij}(\omega)$ for $\Gamma_{ij}(\omega, \mathbf{r}_i, \mathbf{r}_j)$ and $\Delta_{ij}(\omega, \mathbf{r}_i, \mathbf{r}_j)$ respectively.

From equations 2.12a to 2.14a of reference [80], it is easy to see that if $\{\mathbf{E}_n(\mathbf{r})\}$ compose a complete set of eigen mode, $\{\mathbf{E}_n^*(\mathbf{r})\}$ is also a complete set of eigen mode. Then

$$\Gamma_{ij}(\omega) = s_{i,j}(\omega) \sum_n \mathbf{E}_n^*(\mathbf{r}_i)\cdot\hat{\mathbf{u}}_i\mathbf{E}_n(\mathbf{r}_j)\cdot\hat{\mathbf{u}}_j\delta(\omega - \omega_n). \quad (10)$$

could also be written as:

$$\Gamma_{ij}(\omega) = s_{i,j}(\omega) \sum_n \mathbf{E}_n(\mathbf{r}_i)\cdot\hat{\mathbf{u}}_i\mathbf{E}_n^*(\mathbf{r}_j)\cdot\hat{\mathbf{u}}_j\delta(\omega - \omega_n). \quad (11)$$

So we have :

$$\Gamma_{ij}(\omega) = \frac{s_{i,j}(\omega)}{2} \sum_n [\mathbf{E}_n(\mathbf{r}_i)\cdot\hat{\mathbf{u}}_i\mathbf{E}_n^*(\mathbf{r}_j)\cdot\hat{\mathbf{u}}_j + h.c.] \delta(\omega - \omega_n). \quad (12)$$

Once we get the cooperative decay parameters $\Gamma_{ij}(\omega)$, the dipole-dipole interaction potential $\Delta_{ij}(\omega)$ can be achieved through Eq. (8c).

III. METHOD

Here we propose a new method to rigorously get the cooperative decay parameters based on finite-difference

time domain algorithm. We show that dipole-dipole interaction can be got through calculating the collective and individual radiation rates of classical dipoles. We begin with Maxwell equations:

$$\begin{aligned}\nabla \times \mathbf{E}(\mathbf{r}, t) &= -\frac{\partial \mathbf{B}(\mathbf{r}, t)}{\partial t}, \\ \nabla \times \mathbf{B}(\mathbf{r}, t) &= \mu_0 \varepsilon(\mathbf{r}) \frac{\partial \mathbf{E}(\mathbf{r}, t)}{\partial t} + \mu_0 \frac{\partial \mathbf{P}(\mathbf{r}, t)}{\partial t}, \\ \nabla \cdot \varepsilon(\mathbf{r}) \mathbf{E}(\mathbf{r}, t) &= \rho(\mathbf{r}, t), \\ \nabla \cdot \mathbf{B}(\mathbf{r}, t) &= 0.\end{aligned}\quad (13)$$

Expand $\mathbf{E}(\mathbf{r}, t) = \sum_n \alpha_n(t) \mathbf{E}_n(\mathbf{r})$ where $\mathbf{E}_n(\mathbf{r})$ is the same as the eigen modes at the quantum analysis section. If we let $\mathbf{P}(\mathbf{r}, t) = e^{-i\omega_0 t} \mathbf{u}(\mathbf{r})$, then $\alpha_n(t)$ satisfies the following equation:

$$\ddot{\alpha}_n(t) + \omega_n^2 \alpha_n(t) = -\omega_0^2 e^{-i\omega_0 t} \int d\mathbf{r} \mathbf{u}(\mathbf{r}) \cdot \mathbf{E}_n^*(\mathbf{r}). \quad (14)$$

Through Eq. (14), we get:

$$\alpha_n(t) = \lim_{\eta \rightarrow 0^+} \frac{-\omega_0^2 \exp(-i\omega_0 t)}{\omega_n^2 - \omega_0^2 + i\eta} \int d\mathbf{r} \mathbf{u}(\mathbf{r}) \cdot \mathbf{E}_n^*(\mathbf{r}). \quad (15)$$

If $\mathbf{u}(\mathbf{r}) = \sum_i \hat{\mathbf{u}}_i \delta(\mathbf{r} - \mathbf{r}_i)$, the emission power is given by

$$P(\omega_0) = \frac{\pi}{4} \omega_0^2 \sum_n \left| \sum_i \hat{\mathbf{u}}_i \cdot \mathbf{E}_n^*(\mathbf{r}_i) \right|^2 \delta(\omega_0 - \omega_n). \quad (16)$$

In the two dipoles instance, i.e., $i = A, B$, the total power is

$$P^{AB}(\omega_0) = \frac{\pi}{4} \omega_0^2 \sum_n \left| \sum_{i=A,B} \hat{\mathbf{u}}_i \cdot \mathbf{E}_n^*(\mathbf{r}_i) \right|^2 \delta(\omega_0 - \omega_n). \quad (17)$$

If there is only one dipole, i.e., $i = A$ or $i = B$, then

$$P^A(\omega_0) = \frac{\pi}{4} \omega_0^2 \sum_n \left| \hat{\mathbf{u}}_A \cdot \mathbf{E}_n^*(\mathbf{r}_A) \right|^2 \delta(\omega_0 - \omega_n), \quad (18)$$

$$P^B(\omega_0) = \frac{\pi}{4} \omega_0^2 \sum_n \left| \hat{\mathbf{u}}_B \cdot \mathbf{E}_n^*(\mathbf{r}_B) \right|^2 \delta(\omega_0 - \omega_n). \quad (19)$$

Combining Eq. (17), Eq. (18) and Eq. (19), we define the cooperative emission power as:

$$\begin{aligned}P_{co}(\omega_0) &\equiv P^{AB}(\omega_0) - P^A(\omega_0) - P^B(\omega_0), \\ &= \frac{\pi \omega_0^2}{4} \sum_n [\hat{\mathbf{u}}_A \cdot \mathbf{E}_n^*(\mathbf{r}_A) \hat{\mathbf{u}}_B \cdot \mathbf{E}_n(\mathbf{r}_B) + \\ &\quad h.c.] \delta(\omega_0 - \omega_n).\end{aligned}\quad (20)$$

Through Eq. (20) and Eq. (12), we found that:

$$\frac{\Gamma_{ij}^c(\omega)}{\Gamma_{ii}^0(\omega)} = \frac{\mu_i \mu_j \omega_i \omega_j}{\mu_i^2 \omega_i^2} \frac{P_{co}^c(\omega)}{2P_0^v(\omega)}. \quad (21)$$

where $\Gamma_{ij}^c(\omega)$ and $P_{co}^c(\omega)$ correspond to cooperative decay parameters and cooperative emission power of two unit classical dipoles in complex environment. $P_0^v(\omega)$ correspond to the emission power of a unit classical dipole in vacuum. $\Gamma_{ii}^0(\omega)$ is the local coupling strength for a two level atom with transition dipole moment \mathbf{u}_i and transition frequency of bare atom ω_i in vacuum. Using the result of [8], we get $\Gamma_{ii}^0(\omega)/(u_i^2 \omega_i^2) = \omega/(3\pi \varepsilon_0 \hbar c^3)$.

In order to make the cooperative decay parameters more clearly, we define

$$\begin{aligned}\eta(\omega) &\equiv \frac{P_{co}^c(\omega)}{2P_0^v(\omega)}, \\ \alpha_i &\equiv \frac{u_i^2 \omega_i^2}{3\pi \varepsilon_0 \hbar c^3}.\end{aligned}\quad (22)$$

where α_i is totally decided by the two level atom i . Then we get

$$\Gamma_{ij}^c(\omega) = \sqrt{\alpha_i \alpha_j} \eta(\omega) \omega. \quad (23)$$

Equation. (23) is the main content of our method. $\eta(\omega)$ can be obtained through calculating $P_{co}^c(\omega)$ and $P_0^v(\omega)$ by FDTD method. Utilizing Eq. (8c), we can get the dipole-dipole interaction potential $\Delta_{ij}(\omega)$. Furthermore, we see that our method may be generalized to study many dipole interactions through this similar procedure.

IV. NUMERICAL RESULTS AND DISCUSSION

A. Cooperative decay parameters in vacuum and planar microcavity

Before applying our method to investigate dipole-dipole interaction in photonic crystal nanocavity, we first numerically validate our approach in the case for dipoles in vacuum or planar microcavity where analytic expression for the cooperative decay parameters $\Gamma_{ij}^c(\omega)$ can be easily got through mode-expansion method. In this section, for simplicity, we set $\omega_A = \omega_B = \omega_0$ and $\alpha_A = \alpha_B = \alpha_0 = \omega_0^2 u_i^2 / 3\pi \varepsilon_0 \hbar c^3$. In vacuum, the two transition dipole moments are parallel to the x axis and the interatomic separation axis is along the z axis. The eigen-function of vacuum reads $\mathbf{E}_{\mathbf{k},l}(\mathbf{r}) = \hat{\mathbf{e}}_{\mathbf{k}}^l e^{i\mathbf{k} \cdot \mathbf{r}}$. Inserting this into Eq. (12) and making use of $\sum_{l=1,2} \hat{\mathbf{e}}_{\mathbf{k},i}^l \hat{\mathbf{e}}_{\mathbf{k},j}^l = \delta_{ij} - \hat{\mathbf{k}}_i \hat{\mathbf{k}}_j$, we get the analytic cooperative decay parameters $\Gamma_{ij}(\omega)$:

$$\Gamma_{ij}(\omega) = \frac{3\omega \Gamma_0(\omega_0)}{2\omega_0} \left[\frac{\sin(\omega R/c)}{(\omega R/c)} + \frac{\cos(\omega R/c)}{(\omega R/c)^2} - \frac{\sin(\omega R/c)}{(\omega R/c)^3} \right]. \quad (24)$$

where $R = |\mathbf{r}_i - \mathbf{r}_j|$ is the distance between the two dipoles. If $R = 0$, for the two dipole located at the

same place, $\Gamma_{ij}(\omega_0) = \Gamma_0(\omega_0) = \omega_0^3 u_i^2 / 3\pi\epsilon_0 \hbar c^3$ which is the radiation rate of the dipole in vacuum. We set $\omega = \omega_0 = 2\pi c/\lambda$ and increase the interatomic separation R to simplify our discussion. In Fig. 2, black line is for the analytic results (Eq. (24)) and red boxed dots represent the calculated results (Eq. (23)). It can be clearly seen that $\Gamma_{ij}(\omega)$ got through our method agrees very well with the analytic results.

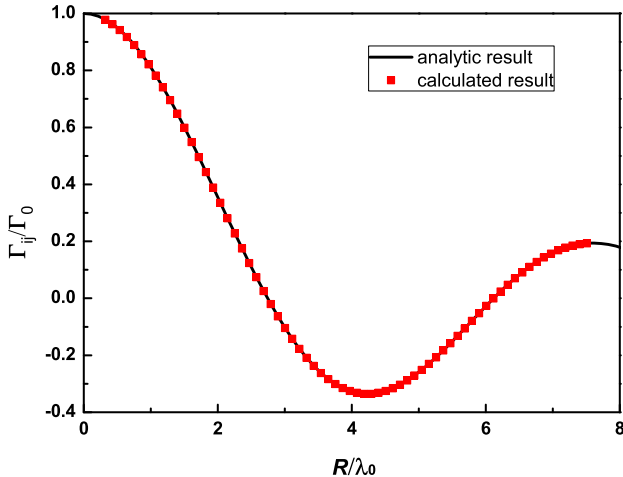


FIG. 2: (Color online). Comparison between our numerical results and the analytic results of cooperative decay parameters for dipoles located in vacuum. Cooperative decay parameters Γ_{ij}/Γ_0 as a function of the interatomic separation R/λ_0 when $\omega = \omega_0 = 2\pi c/\lambda_0$; Black line is for the analytic results (Eq. (24)) and red boxed dots represent the calculated results (Eq. (23)). The orientation of the two transition dipole moments are the same and perpendicular to their separation.

Similar result is also got when the two point dipoles are located in a planar nanocavity. Here, the cooperative decay parameters $\Gamma_{ij}(\omega)$ could also be got analytically. The structure is shown in Fig. 3(a). The origin is at the center for x, y axis and at the bottom conductor for z axis. The CPML encloses the domain, as can be seen from the top view at the right-hand side. The orientation of the two transition dipole moments are the same and along z (red arrowhead). They are arranged along x axis and their separation is R . The analytic cooperative decay parameter $\Gamma_{ij}(\omega)$ for these two dipoles is:

$$\Gamma_{ij}(\omega) = \Gamma_0(\omega_0) \left(\frac{3\lambda_0}{8\pi L} \right) \left\{ \int_0^{2\pi} d\theta \cos\left(\frac{2\pi R}{\lambda} \cos\theta\right) + \sum_{n=1}^{[2L/\lambda]} 2 \left[1 - \left(\frac{n\lambda}{2L} \right)^2 \right] \cos\left(\frac{n\pi z_1}{L}\right) \cos\left(\frac{n\pi z_2}{L}\right) \right\} \times \int_0^{2\pi} d\theta \cos\left(2\pi R \sqrt{\left(\frac{1}{\lambda}\right)^2 - \left(\frac{n}{2L}\right)^2} \cos\theta \right). \quad (25)$$

where $\omega = 2\pi c/\lambda$, $[2L/\lambda]$ is the largest integer less than $2L/\lambda$, $\Gamma_0(\omega_0)$ is spontaneous emission rate in vacuum for any one of the two same dipoles, and z_i is the coordinate

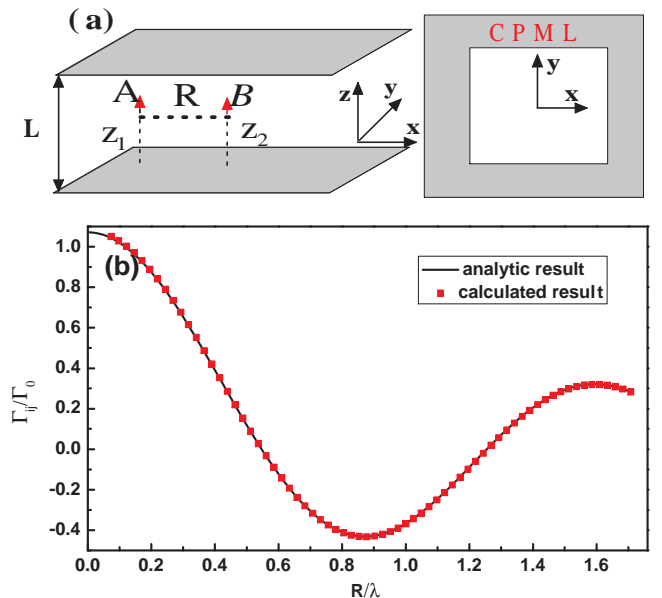


FIG. 3: (Color online). Sketch of setup and the comparison between our numerical results and the analytic results of cooperative decay parameters for dipoles located in vacuum. (a) Schematic diagram of the planar cavity with a top view of the computation domain at the right side. The two dipoles locate at the center. The orientation of the two transition dipole moments are the same and along z (red arrowhead). They are arranged along x axis and their separation is R . (b) Cooperative decay parameters Γ_{ij}/Γ_0 as a function of the interatomic separation R when $z_1 = z_2 = L/2$, $L/\lambda_0 = L/\lambda = 0.7$; black line is for the analytic results from Eq. (25) and red boxed dots represent the calculated from Eq. (23).

of z for dipole i , here, we set $z_1 = z_2 = L/2$, R is the distance between the two dipoles in xy plane. For $R = 0$, this leads to the well-known results

$$\Gamma_z(\omega_0) = \Gamma_0(\omega_0) \left(\frac{3\lambda_0}{4L} \right) \left\{ 1 + \sum_{n=1}^{[2L/\lambda_0]} 2 \left[1 - \left(\frac{n\lambda_0}{2L} \right)^2 \right] \cos^2\left(\frac{n\pi}{2}\right) \right\}. \quad (26)$$

In the calculation, we set $L/\lambda_0 = L/\lambda = 0.7$, and R/L is gradually increased from 0 to 49/41 for simplicity. Cooperative decay parameters Γ_{ij}/Γ_0 as a function of the interatomic separation R is displayed in Fig. 3(b). black line is for the analytic results from Eq. (25) and red boxed dots represent the calculated from Eq. (23). We find that the numerical result from our method also agrees very well with the analytic solution.

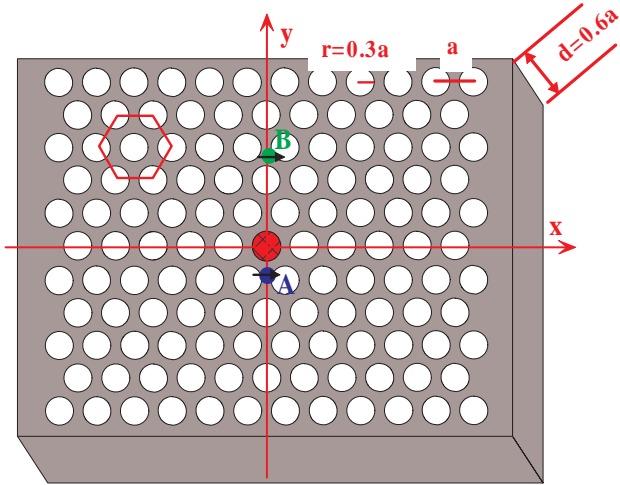


FIG. 4: (Color online). The sketch of the photonic crystal nanocavity. It consists of a thin dielectric slab with air holes arranged as triangular lattice. The lattice constant is a , the radii of the air hole is $r = 0.3a$ and the slab height is $d = 0.6a$. The refractive index of the slab is 3.4. There is a defect hole in the center with refractive index $n_{def} = 2.4$. Its radii is the same as the air hole. The origin of the axes is set at the center of the photonic crystal nanocavity. The two dipoles are located at point A and B on the center plane of the slab and the two dipole moments are parallel to the x axis.

B. Dipole-dipole interaction in photonic crystal nanocavity

Through the above two numerical tests, we clearly shown that our method could be able to efficiently and exactly deal with the dipole-dipole interaction. In the following of this section, dipole-dipole interaction in photonic crystal cavity (PCs) has been numerically studied. The sketch of the photonic crystal cavity is displayed in Fig. 4. It consists of a thin dielectric slab with air holes arranged as triangular lattice. The lattice constant is a , the radii of the air hole is $r = 0.3a$ and the slab height is $d = 0.6a$. The refractive index of the slab is 3.4. There is a defect hole in the center with refractive index $n_{def} = 2.4$. Its radii is the same as the air hole. The two dipoles are located at point A and B on the center plane of the slab and the two dipole moments are parallel to the x axis. The origin of the axes is set at the center of the PCs cavity. For convenience, the special points are also drawn in Fig. 4. ‘Atom’ A located at $(0, -11/15, 0)a$, ‘Atom’ B located $(0, R - 11a/15, 0)$, where R represents the separation and varies from $a/15$ to $50a/15$. The two transition dipole moments are parallel to the x axis. Thanks to the scaling law, the cooperative decay parameters $\Gamma_{ij}(\omega)$, dipole-dipole interaction potential $\Delta_{ij}(\omega)$ and frequency ω in unit of $2\pi c/a$ are dimensionless.

The frequency dependent characters for cooperative

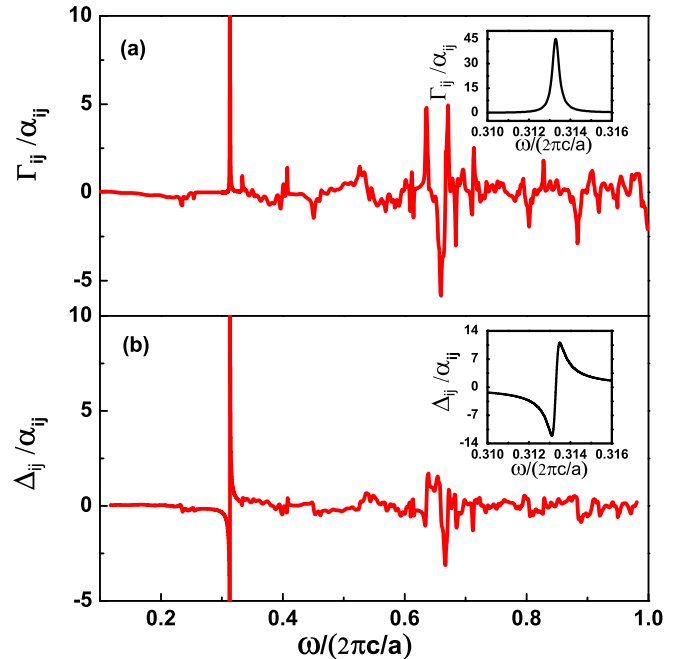


FIG. 5: (Color online). The frequency dependent characters for cooperative decay parameters and dipole-dipole interaction potential. (a) The cooperative decay parameters $\Gamma_{ij}(\omega)$ and (b) the dipole-dipole interaction potential $\Delta_{ij}(\omega)$ versus ω for atom A located at $(0, -11/15, 0)a$, atom B located at $(0, 11/15, 0)a$ in the photonic crystal nanocavity. $\Gamma_{ij}(\omega)$ and $\Delta_{ij}(\omega)$ are in unit of α_{ij} ($\alpha_{ij} \equiv \sqrt{\alpha_i \alpha_j} 2\pi c/a$). The ω is in unit of $2\pi c/a$. The two dipole moments are parallel and along the x axis. The insets show the behavior around the defect frequency ($\omega_c = 0.3133(2\pi c/a)$) of the cavity. The two transition dipoles are parallel and along the x axis.

decay parameters $\Gamma_{ij}(\omega)$ and dipole-dipole interaction potential $\Delta_{ij}(\omega)$ are presented in Fig. 5(a) and Fig. 5(b) for atom A located at $(0, -11/15, 0)a$ and atom B located at $(0, 11/15, 0)a$. The insets show the behaviors for frequency around the resonance frequency ($\omega_c = 0.3133(2\pi c/a)$). From Fig. 5(a), we clearly see that $\Gamma_{ij}(\omega)$ oscillates remarkably when ω is far away from ω_c , which shows the powerful modulation ability of photonic crystal for the electromagnetic eigen mode and the density of photonic states. For $\omega = \omega_c$ (the inset), $\Gamma_{ij}(\omega_c) \approx 144\Gamma_0$ for relatively large atomic separation ($R \approx 0.46\lambda_0$), where Γ_0 is the largest $\Gamma_{ij}(\omega_0)$ for two dipoles located in vacuum for the atomic separation $R = 0$. This large Γ_{ij} is attributed to the enhancement of photon emission and reabsorbing rates, which can be roughly characterized by the ratio of Q/V . Aimed for quantum computation and quantum information processing [58, 59] where large Γ_{ij} or large Δ_{ij} is needed, we can increase the quality factor Q through improving the nanocavity design. For $\omega \sim \omega_c$ (the inset), $\Gamma_{ij}(\omega)$ varies sharply and is sensitive to the frequency. This implies that tuning ω_c of the cavity or ω_i of the dipole can both

help to control Γ_{ij} . Figure 5(b) shows similar properties for the dipole-dipole interaction potential. The inset shows that repulsive or attractive potential can be got around the cavity frequency.

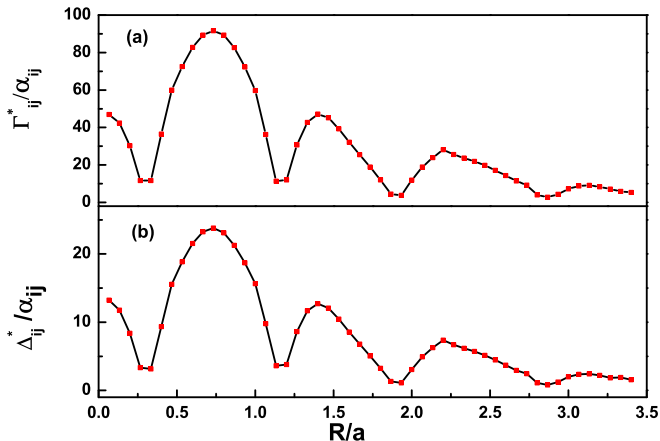


FIG. 6: (Color online). The position dependent characteristics for cooperative decay parameters and dipole-dipole interaction potential. (a) The absolute maximum cooperative decay parameters $\Gamma_{ij}^* = |\Gamma_{ij}|$ and (b) the absolute maximum dipole-dipole interaction potential $\Delta_{ij}^* = |\Delta_{ij}|$ versus the interatomic separation R for atom A located at $(0, -11/15, 0)a$ and atom B located at $(0, R - 11a/15, 0)$ in the PCs cavity. The maximum are calculated for ω around ω_c . Γ_{ij}^* and Δ_{ij}^* are in unit of α_{ij} ($\alpha_{ij} \equiv \sqrt{\alpha_i \alpha_j} \sqrt{2\pi c/a}$) and ω is in unit of $2\pi c/a$. The two transition dipoles are parallel and along the x axis.

The position dependent characters have been investigated. Figure 6(a) and 6(b) show the absolute maximum value for ω around ω_c of cooperative decay parameters $\Gamma_{ij}^* = |\Gamma_{ij}|$ and dipole-dipole interaction potential $\Delta_{ij}^* = |\Delta_{ij}|$ as a function of their separation R (atom A located at $(0, -11a/15, 0)$ and atom B located at $(0, R - 11a/15, 0)$) are show where the maximum are calculated for ω around ω_c . Γ_{ij}^* and Δ_{ij}^* are in unit of α_{ij} ($\alpha_{ij} \equiv \sqrt{\alpha_i \alpha_j} \sqrt{2\pi c/a}$). The ω is in unit of $2\pi c/a$. The maximum value Γ_{ij}^* and Δ_{ij}^* varies in a similar way except for the amplitude. The above phenomena can be understood as follows: Γ_{ij}^* depends much on the electric field of the defect mode. Equation (12) shows that Γ_{ij}^* changes in the same way as the electric field of the cavity mode at the location of atom B. The cavity mode along the y axis looks much the same as Fig. 6(a) and we did not show it here. Further, we clearly see that $\Gamma_{ij}^* = \Gamma_{ii}^*$ and $\Delta_{ij}^* = \Delta_{ii}^*$ have been realized for atom A and atom B located at positions with same electric field strength along the x axis.

V. CONCLUSION

In summary, we have proposed a new efficient and rigorous numerical method to investigate dipole-dipole interaction in photonic crystal nanocavity. We calculate the collective and individual radiation rates of classical dipoles by directly solving Maxwell's equations in real space with a free-space boundary condition. By using the result of two dipoles radiation rate minus the sum of the two individual radiation rates, we get the cooperative decay parameters and dipole-dipole interaction potential. Through the self-consistent procedure (Eq. (6)), exact non-Markov results can be got and both real and virtual photon effects have been taken into account. Further, it can be applied for dipoles with different transition frequencies in both weak and strong coupling regimes. Our investigation suggests that this method works well for dipoles located in media with arbitrary shape and may be generalized to calculate many dipoles interaction. Numerical validation has been made in vacuum and planar nanocavity. Both results agree very well with the analytic.

Applying this method to a simple photonic crystal nanocavity, it is found that the cooperative decay parameters and the dipole-dipole interaction potential strongly depend on the atomic position, the transition frequency, quality factor and the cavity frequency. For two dipoles arranged at positions with the same local coupling strength, the cooperative decay parameters is equal to the local coupling strength. Large cooperative decay parameters is achieved at the resonance frequency. Dipole-dipole interaction potential changes continuously from attractive to repulsive case for transition frequency varying in a domain of the cavity linewidth around the resonance frequency. Larger value and sharper change of cooperative parameters and dipole-dipole interaction can be obtained for higher quality factor. Owing to the Photonic crystal nanostructure is one of the most promising platform. It offers many advantages, including high quality factor, small mode volume, integrability with waveguide and fixed position of dipoles. In addition, many ingenious schemes for static and ultra fast dynamic control of the quality factor, resonance frequency have been proposed. Based on these techniques for photonic crystal nanocavity and methods for tuning the transition frequency of quantum dots, our results provide some manipulative approaches for dipole-dipole interaction with potential application in various fields such as quantum computation and quantum information processing based on solid state nanocavity and quantum dot system.

ACKNOWLEDGMENT

This work was supported by NSFC under grants Nos. 10934010, 60978019, the NKBRSF under grants

Nos. 2009CB930701, 2010CB922904, 2011CB921502, 2012CB821300, and NSFC-RGC under grants Nos. 11061160490 and 1386-N-HKU748/10.

* Electronic address: wangxueh@mail.sysu.edu.cn

- [1] E. M. Purcell, *Phys. Rev.* **69**, 681 (1946).
- [2] G. Barton, *Proc. R. Soc. London, Ser. A* **320**, 251 (1970).
- [3] G. S. Agarwal, *Phys. Rev. A* **12**, 1475 (1975).
- [4] R. G. Hulet, E. S. Hilfer, and D. Kleppner, *Phys. Rev. Lett.* **55**, 2137 (1985).
- [5] S. John, *Phys. Rev. Lett.* **58**, 2486 (1987).
- [6] H. Yokoyama, *Science* **256**, 66 (1992).
- [7] S. Scheel, L. Knöll, and D. G. Welsch, *Phys. Rev. A* **60**, 1590 (1999).
- [8] X. H. Wang, B. Y. Gu, R. Z. Wang, and H. Q. Xu, *Phys. Rev. Lett.* **91**, 113904 (2003).
- [9] T. Yoshie, A. Scherer, J. Hendrickson, G. Khitrova, H. M. Gibbs, G. Rupper, C. Ell, O. B. Shchekin, and D. G. Deppe, *Nature (London)* **432**, 200 (2004).
- [10] S. M. Thon, M. T. Rakher, H. Kim, J. Gudat, W. T. M. Irvine, P. M. Petroff, and D. Bouwmeester, *Appl. Phys. Lett.* **94**, 111115 (2009).
- [11] M. L. Andersen, S. Stobbe, A. S. Sørensen, and P. Lodahl, *Nature Physics* **7**, 215 (2011).
- [12] G. Khitrova, H. M. Gibbs, M. Kira, S. W. Koch, and A. Scheerer, *Nature Physics* **2**, 81 (2006).
- [13] K. M. Birnbaum, A. Boca, R. Miller, A. D. Boozer, T. E. Northup, and H. J. Kimble, *Nature (London)* **436**, 87 (2005).
- [14] A. D. Greentree, C. Tahan, J. H. Cole, and L. C. L. Hollenberg, *Nature Physics* **2**, 856 (2006).
- [15] P. Goy, J. M. Raimond, M. Gross, and S. Haroche, *Phys. Rev. Lett.* **50**, 1903 (1983).
- [16] H. Walther, B. T. H. Varcoe, B. G. Englert, and T. Becker, *Rep. Prog. Phys.* **69**, 1325 (2006).
- [17] D. Braun, *Phys. Rev. Lett.* **89**, 277901 (2002).
- [18] K. Panajotov, and M. Dems, *Opt. Lett.* **35**, 829 (2010).
- [19] D. Meschede, H. Walther, and G. Muller, *Phys. Rev. Lett.* **54**, 551 (1985).
- [20] O. Painter, R. K. Lee, A. Scherer, A. Yariv, J. D. Dapkus, J. D. O'Brien, and I. Kim, *Science* **284**, 1819 (1999).
- [21] S. Noda, *Science* **314**, 260 (2006).
- [22] R. H. Lehmberg, *Phys. Rev. A* **2**, 883 (1970).
- [23] G. S. Agarwal, and A. K. Patnaik, *Phys. Rev. A* **63**, 043805 (2001).
- [24] C. Hettich, C. Schmitt, J. Zitzmann, S. Kühn, I. Gerhard, and V. Sandoghdar, *Science* **298**, 385 (2002).
- [25] H. Y. Lu, H. Lu, J. N. Zhang, R. Z. Qiu, H. Pu, and S. Yi, *Phys. Rev. A* **82**, 023622 (2010).
- [26] E. V. Goldstein, and P. Meystre, *Phys. Rev. A* **56**, 5153 (1997).
- [27] T. Kobayashi, Q. B. Zheng, and T. Sekiguchi, *Phys. Rev. A* **52**, 2835 (1995).
- [28] R. H. Lehmberg, *Phys. Rev. A* **2**, 889 (1970).
- [29] G. S. Agarwal, and S. D. Gupta, *Phys. Rev. A* **57**, 667 (1998).
- [30] S. Rist, J. Eschner, M. Hennrich, and G. Morigi, *Phys. Rev. A* **78**, 013808 (2008).
- [31] L. M. Folan, S. Arnold, and S. D. Druger, *Chem. Phys. Lett.* **118**, 322 (1985).
- [32] S. Bay, P. Lambropoulos, and K. Mølmer, *Phys. Rev. A* **55**, 1485 (1997).
- [33] P. T. Kristensen, J. Mørk, P. Lodahl, and S. Hughes, *Phys. Rev. B* **83**, 075305 (2011).
- [34] E. Gallardo, L. J. Martínez, A. K. Nowak, D. Sarkar, H. P. van der Meulen, J. M. Calleja, C. Tejedor, I. Prieto, D. Granados, A. G. Taboada, J. M. García, and P. A. Postigo, *Phys. Rev. B* **81**, 193301 (2010).
- [35] A. Laucht, J. M. V. Bôas, S. Stobbe, N. Hauke, F. Hofbauer, G. Böhm, P. Lodahl, M. C. Amann, M. Kaniber, and J. J. Finley, *Phys. Rev. B* **82**, 075305 (2010).
- [36] S. Reitzenstein, A. Loeffler, C. Hofman, A. Kubanek, M. Kamp, J. P. Reithmaier, and A. Forchel, *Opt. Lett.* **31**, 1738 (2006).
- [37] S. Weiler, A. Ulhaq, S. M. Ulrich, S. Reitzenstein, A. Löffler, A. Forchel, and P. Michler, *Phys. Rev. B* **82**, 205326 (2010).
- [38] H. Kim, D. Sridharan, T. C. Shen, G. S. Solomon, and E. Waks, *Opt. Exp.* **19**, 2589 (2011).
- [39] A. G. Tudela, D. M. Cano, E. Moreno, L. M. Moreno, C. Tejedor, and F. J. G. Vidal, *Phys. Rev. Lett.* **106**, 020501 (2011).
- [40] F. Zhou, Y. Liu, and Z. Y. Li, *Opt. Lett.* **36**, 1969 (2011).
- [41] D. Dzsotjan, J. Kästel, and M. Fleischhauer, *Phys. Rev. B* **84**, 075419 (2011).
- [42] D. Dzsotjan, A. S. Sørensen, and M. Fleischhauer, *Phys. Rev. B* **82**, 075427 (2010).
- [43] D. M. Cano, L. M. Moreno, F. J. G. Vidal, and E. Moreno, *Nano Lett.* **10**, 3129 (2010).
- [44] Y. P. Yang, J. P. Xu, H. Chen, and S. Y. Zhu, *Phys. Rev. A* **82**, 030304(R) (2010).
- [45] J. P. Xu, M. A. Amri, Y. P. Yang, S. Y. Zhu, and M. S. Zubairy, *Phys. Rev. A* **84**, 032334 (2011).
- [46] Y. Takahashi, H. Hagino, Y. Tanaka, B. Song, T. Asano, and S. Noda, *Opt. Exp.* **15**, 17206 (2007).
- [47] Y. Tanaka, T. Asano, and S. Noda, *J. Lightw. Technol.* **26**, 0733 (2008).
- [48] S. Vignolini, F. Intonti, F. Riboli, L. Balet, L. H. Li, M. Francardi, A. Gerardino, A. Fiore, D. S. Wiersma, and M. Gurioli, *Phys. Rev. Lett.* **105**, 123902 (2010).
- [49] S. Mosor, J. Hendrickson, B. C. Richards, J. Sweet, G. Khitrova, H. M. Gibbs, T. Yoshie, A. Scherer, O. B. Shchekin and D. G. Deppe, *Appl. Phys. Lett.* **87**, 141105 (2005).
- [50] M. Burrelli, T. Kampfrath, D. van Oosten, J. C. Prangsma, B. S. Song, S. Noda, and L. Kuipers, *Phys. Rev. Lett.* **105**, 123901 (2010).
- [51] Y. Tanaka, J. Upham, T. Nagashima, T. Sugiya, T. Asano, and S. Noda, *Nat. Mat.* **6**, 862 (2007).
- [52] T. Tanabe, M. Notomi, H. Taniyama, and E. Kuramochi, *Phys. Rev. Lett.* **102**, 043907 (2009).
- [53] K. D. Jöns, R. Hafenbrak, R. Singh, F. Ding, J. D. Plumhof, A. Rastelli, O. G. Schmidt, G. Bester, and P. Michler, *Phys. Rev. Lett.* **107**, 217402 (2011).
- [54] A. Faraon, A. Majumdar, H. Kim, P. Petroff, and J. Vučković, *Phys. Rev. Lett.* **104**, 047402 (2010).
- [55] S. Reitzenstein, S. Münch, P. Franek, A. R. Iman, A. Löffler, S. Höfling, L. Worschech, and A. Forchel, *Phys. Rev. Lett.* **103**, 127401 (2009).
- [56] S. Karaveli, and R. Zia, *Phys. Rev. Lett.* **106**, 193004 (2011).

- [57] M. D. Lukin, and P. R. Hemmer, *Phys. Rev. Lett.* **84**, 28181 (2000).
- [58] M. D. Lukin, M. Fleischhauer, R. Cote, L. M. Duan, D. Jaksch, J. I. Cirac, and P. Zoller, *Phys. Rev. Lett.* **87**, 037901 (2001).
- [59] D. Jaksch, J. I. Cirac, and P. Zoller, S. L. Rolston, R. Côté and M. D. Lukin, *Phys. Rev. Lett.* **85**, 2208 (2000).
- [60] L. Isenhower, E. Urban, X. L. Zhang, A. T. Gill, T. Henage, T. A. Johnson, T. G. Walker, and M. Saffman, *Phys. Rev. Lett.* **104**, 010503 (2010).
- [61] S. B. Zheng, and G. C. Guo, *Phys. Rev. Lett.* **85**, 2392 (2000).
- [62] S. Hughes, *Phys. Rev. Lett.* **94**, 227402 (2005).
- [63] P. Yao, and S. Hughes, *Opt. Exp.* **17**, 11505 (2009).
- [64] A. G. Tudela, D. M. Cano, E. Moreno, L. M. Moreno, C. Tejedor, and F. J. G. Vidal, *Phys. Rev. Lett.* **106**, 020501 (2011).
- [65] J. Ruostekoski, and J. Javanainen, *Phys. Rev. A* **55**, 513 (1997).
- [66] H. Y. Xie, H. Y. Chung, P. T. Leung, and D. P. Tsai, *Phys. Rev. B* **80**, 155448 (2009).
- [67] Y. K. Youl, C. K. Cheol, and A. C. Won, *Opt. Exp.* **17**, 11495(2009).
- [68] I. E. Protsenko, A. V. Uskov, O. A. Zaimidoroga, V. N. Samoilov, and E. P. O'Reilly, *Phys. Rev. A* **71**, 063812 (2005).
- [69] A. Reinhard, K. C. Younge, T. C. Liebisch, B. Knuffman, P. R. Berman, and G. Raithel, *Phys. Rev. Lett.* **100**, 233201 (2008).
- [70] T. A. Johnson, E. Urban, T. Henage, L. Isenhower, D. D. Yavuz, T. G. Walker, and M. Saffman, *Phys. Rev. Lett.* **100**, 113003 (2008).
- [71] N. Saquet, A. Cournol, J. Beugnon, J. Robert, P. Pillet, and N. Vanhaecke, *Phys. Rev. Lett.* **104**, 133003 (2010).
- [72] M. Harlander, R. Lechner, M. Brownnutt, R. Blatt, W. Hänsel, *Nature* **471**, 200 (2011)
- [73] M. H. G. de Miranda, A. Chotia1, B. Neyenhuis, D. Wang, G. Quéméner, S. Ospelkaus, J. L. Bohn, J. Ye, and D. S. Jin, *Nature Phys.* **7**, 502 (2011).
- [74] S. I. Schmid, and J. Evers, *Phys. Rev. A* **77**, 013822 (2008).
- [75] J. P. Dowling, and C. M. Dowden, *Phys. Rev. A* **46**, 612 (1992).
- [76] Y. Xu, R. K. Lee, and A. Yariv, *Phys. Rev. A* **61**, 033807 (2000).
- [77] J. K. Hwang, H. Y. Ryu, and Y. H. Lee, *Phys. Rev. B* **60**, 4688 (1999).
- [78] W. H. Louisell, *Quantum Statistical Properties of Radiation* (John Wiley & Sons, New York, 1973).
- [79] C. C. Tannoudji, J. D. Poc, and G. Grynberg, *Atom-Photon Interactions: Basic Processes and Application* (John Wiley & Sons, New York, 1992).
- [80] R. J. Glauber, and M. Lewenstein, *Phys. Rev. A* **43**, 467 (1991).